

Experimental investigation of electrode cycle performance and electrochemical kinetic performance under stress loading

Zi-Han Liu(刘子涵), Yi-Lan Kang(亢一澜), Hai-Bin Song(宋海滨), Qian Zhang(张茜), and Hai-Mei Xie(谢海妹)‡
Citation: Chin. Phys. B, 2021, 30 (**1**): 016201. DOI: 10.1088/1674-1056/abb30e
Journal homepage: http://cpb.iphy.ac.cn; http://iopscience.iop.org/cpb

What follows is a list of articles you may be interested in

Structural, mechanical, and electronic properties of Zr-Te compounds from first-principles calculations

Peng Wang(王鹏), Ning-Chao Zhang(张宁超), Cheng-Lu Jiang(蒋城露), Fu-Sheng Liu(刘福生), Zheng-Tang Liu(刘正堂), Qi-Jun Liu(刘其军)
Chin. Phys. B, 2020, 29 (**7**): 076201. DOI: 10.1088/1674-1056/ab8da7

Surperhard monoclinic BC_6N allotropes: First-principles investigations

Nian-Rui Qu(屈年瑞), Hong-Chao Wang(王洪超), Qing Li(李青), Yi-Ding Li(李一鼎), Zhi-Ping Li(李志平), Hui-Yang Gou(缑慧阳), Fa-Ming Gao(高发明)
Chin. Phys. B, 2019, 28 (**9**): 096201. DOI: 10.1088/1674-1056/ab3439

Nanosheet-structured B_4C with high hardness up to 42 GPa

Chang-Chun Wang(王常春), Le-Le Song(宋乐乐)
Chin. Phys. B, 2019, 28 (**6**): 066201. DOI: 10.1088/1674-1056/28/6/066201

First-principles investigations on structural stability, mechanical, and thermodynamic properties of LaT_2Al_{20} (T=Ti, V, Cr, Nb, and Ta) intermetallic cage compounds

Shanyu Quan(权善玉), Xudong Zhang(张旭东), Cong Liu(刘聪), Wei Jiang(姜伟)
Chin. Phys. B, 2018, 27 (**12**): 126201. DOI: 10.1088/1674-1056/27/12/126201

Influence of high pulsed magnetic field on tensile properties of TC4 alloy

Gui-Rong Li(李桂荣), Fang-Fang Wang(王芳芳), Hong-Ming Wang(王宏明), Rui Zheng(郑瑞), Fei Xue(薛飞), Jiang-Feng Cheng(程江峰)
Chin. Phys. B, 2017, 26 (**4**): 046201. DOI: 10.1088/1674-1056/26/4/046201

Experimental investigation of electrode cycle performance and electrochemical kinetic performance under stress loading*

Zi-Han Liu(刘子涵), Yi-Lan Kang(亢一澜), Hai-Bin Song(宋海滨), Qian Zhang(张茜)†, and Hai-Mei Xie(谢海妹)‡

Tianjin Key Laboratory of Modern Engineering Mechanics, School of Mechanical Engineering, Tianjin University, Tianjin 300350, *China*

(Received 12 July 2020; revised manuscript received 7 August 2020; accepted manuscript online 27 August 2020)

Lithium-ion batteries suffer from mechano–electrochemical coupling problems that directly determine the battery life. In this paper, we investigate the electrode electrochemical performance under stress conditions, where seven tensile/compressive stresses are designed and loaded on electrodes, thereby decoupling mechanics and electrochemistry through incremental stress loads. Four types of multi-group electrochemical tests under tensile/compressive stress loading and normal package loading are performed to quantitatively characterize the effects of tensile stress and compressive stress on cycle performance and the kinetic performance of a silicon composite electrode. Experiments show that a tensile stress improves the electrochemical performance of a silicon composite electrode, exhibiting increased specific capacity and capacity retention rate, reduced energy dissipation rate and impedances, enhanced reactivity, accelerated ion/electron migration and diffusion, and reduced polarization. Contrarily, a compressive stress has the opposite effect, inhibiting the electrochemical performance. The stress effect is nonlinear, and a more obvious suppression via compressive stress is observed than an enhancement via tensile stress. For example, a tensile stress of 675 kPa increases diffusion coefficient by 32.5%, while a compressive stress reduces it by 35%. Based on the experimental results, the stress regulation mechanism is analyzed. Tensile stress loads increase the pores of the electrode material microstructure, providing more deformation spaces and ion/electron transport channels. This relieves contact compressive stress, strengthens diffusion/reaction, and reduces the degree of damage and energy dissipation. Thus, the essence of stress enhancement is that it improves and optimizes diffusion, reaction and stress in the microstructure of electrode material as well as their interactions via physical morphology.

Keywords: prestress loading, silicon composite electrode, tensile stress enhancement, compressive stress suppression

PACS: 62.20.–x, 82.47.Aa, 46.80.+j, 65.40.gk **DOI:** 10.1088/1674-1056/abb30e

1. Introduction

With the rapid development of industry, the demand for high-energy, high-efficiency, long-life lithium-ion batteries (LIBs) is increasing. However, LIBs suffer from mechano–electrochemical multi-field coupling problems in electrode structures, and materials.[1–4] Specifically, the electrochemical lithiation–delithiation process induces electrode stress and fracture failure that affects the electrochemical diffusion and reaction, which directly determines the cycle performance and lifetime degradation of LIBs.[5–8] Thus, the development of high-performance electrode materials and the optimization of the cycle performance and battery life is dependent on studying stress regulation during an electrochemical process and analyzing the influence mechanism of tensile/compressive stresses on the electrochemistry.

Focusing on the mechano–electrochemical coupling problems in LIBs, previous studies have presented theoretical modeling and experimental characterization of electrode mechanical behavior in the lithiation–delithiation process, reporting the electrode deformation, strain, stress, and fracture.[3,5,9–12] Furthermore, electrode cycle performance has been improved by using nanoscale electrode materials, core–shell structure nanomaterials, porous structure materials, surface coatings, *etc*.[13–15] Importantly, current research has shown that the mechanics affects the electrochemical performance and life.[5,16–19] To understand how the mechanics affects the electrochemistry through using theoretical model and numerical simulation, the electrochemical process has been treated as a thermal expansion process. In this way, a theoretical framework coupling deformation and diffusion was built to capture the electrochemical and mechanical parameters, and thereby providing the relation between stress/strain and diffusion, potential and specific capacity. For example, first-principle calculations and density functional theory were applied to Li ion migration energy barriers and the diffusion coefficient under varying mechanical load,[20,21] which show that tensile stress enhances the diffusion within the silicon material while compressive stress inhibits it.[21] Jin *et al.*[22] showed that compressive stress hinders the lithiation–delithiation process of the silicon material and causes a higher overpotential, impeding complete lithiation. Burebi *et al.*[23] found that the stress-regulated lithiation reaction at the interface serves

*Project supported by the Major Program of the National Natural Science Foundation of China (Grant No. 11890680) and the National Natural Science Foundation of China (Grant No. 12022205).

†Corresponding author. E-mail: zhangqian@tju.edu.cn

‡Corresponding author. E-mail: xiehaimei@tju.edu.cn

© 2021 Chinese Physical Society and IOP Publishing Ltd

as a "brake" to reduce the interface velocity and mitigate the lithiation-induced stresses. Lu *et al.*[24] and Gao *et al.*[25] showed that the compressive stress causes the electrode damage to increase and the cycle performance to decrease. Owing to the coupling of electrochemistry and mechanics, however, relatively few experimental studies have reported the relationship between them. On a microscopic scale, transmission electron microscopy can be used to study the relationship between stress and diffusion/reaction. Using this method, McDowell *et al.*[26] showed that coupled compressive stress causes the lithiation of nanoparticles to slow down. Also, Lee *et al.*[27] observed that the contact compressive stress limits the reaction kinetics. And, via the observation of bending germanium/silicon nanowires, Gu *et al.*[28] and Yang *et al.*[29] found that the diffusion on the tensile side of the wires is faster than that on the compressive side. On a macroscale, the relationship between external mechanics and electrochemical performance of commercial electrodes has been characterized by conventional electrochemical tests. For example, Piper *et al.*[30] showed that normal compressive stress causes limited lithiation of a silicon composite electrode, thus exhibiting a higher overpotential and lower specific capacity. Ratyński *et al.*[31] found that the specific capacity of a silicon composite electrode is greater under a larger compressive stress in a certain range. Cannarella and Arnold [32] studied the influence of mechanical loading on battery life by monitoring stacking pressure and capacity during a cycle. Wünsch *et al.*[33] demonstrated that different bracing mechanical conditions affect cell aging. Müller *et al.*[34] reported that the flexible compression within a certain range improves the cycle performance and alleviates aging. Finally, some studies showed that stress affects the electrochemical process parameters such as charge transfer resistance.[33,34] Limited by the experimental technology and loading devices, most experimental researches have been performed under compressive stress. Recently, Xie *et al.*[35] introduced the design of a prestressed battery structure to achieve tensile stress loading, thereby experimentally demonstrating that tensile stress enhances the electrochemical performance of silicon composite electrodes.

In a word, theoretical and numerical simulations have predicted partial relationship between stress and electrochemical parameters, while the coupling effect between mechanics and electrochemistry poses challenges for experimental exploration. The key factor is to separate out the stress effects contained in the experimental results. And it is difficult to quantitatively characterize the effect of stress on the cycling and kinetics performance, and especially to distinguish the role of the tensile stress and compressive stress. All of these limit our understanding of the influence of stress on electrochemistry, thereby limiting the application of mechanic regulation technologies in the development of high-performance electrode materials and the performance optimization of energy storage devices.

In this paper, the electrode cycling performance and kinetic performance under stress loading are experimentally investigated by using an active stress loading method. Four sets of gasket pairs with different curvatures are designed to apply seven different tensile/compressive stresses to the electrodes inside coin-cell batteries. This operation separates the effects of tensile/compressive loads via incremental stress loads. Then, a mechano–electrochemical highly-coupled silicon composite electrode is selected to carry out the experiments. The cycle performance, reaction and diffusion performance under varying tensile/compressive stress are measured by constant-current charge-discharge cycle test, cyclic voltammetry (CV), electrochemical impedance spectroscopy (EIS), and galvanostatic intermittent titration technique (GITT). Finally, the enhancement/inhibition mechanism of the stress loading on the electrochemical performance is discussed. This work provides a scientific basis for the electrochemical regulation of new types of high specific capacity electrode materials.

2. The electrochemical experimental design and measurement under stress loading

2.1. Experimental design of tensile/compressive stress loading

The purpose of this paper is to decouple the effect of mechanics and the effect of electrochemistry via active stress loading, and to further distinguish between the effect of the tensile stress and the effect of compressive stress on the electrode electrochemical performance. First, a stress loading device was designed, wherein a bent gasket pair was used to load the tensile stress and compressive stress on electrodes inside a coin-cell battery. Figure 1(a) shows the structure schematic of a modified 2050-type coin-cell battery, in which each gasket pair consists of a convex and a concave copper gasket with equivalent curvature values and opposite directions, respectively corresponding to a positive and negative curvature. With this design, additional stress was applied to the electrodes through clamping the electrodes into a curved state by means of a bent gasket pair. The equivalent tensile and compressive stress were loaded by changing the contact position between the electrode and a positive and negative curvature gasket, respectively. Specifically, when contacting a positive or negative curvature gasket, the electrode undergoes a tensile or compressive stress as shown in Fig. 1(b). To thoroughly explore the effect of stress on the electrochemical performance, we set three loading programs for tensile stress loading, compressive stress loading, and normal package loading, whose details are shown in Table 1. The device included three groups of curved gasket pairs with curvatures of $k = \pm 45$, ± 30, and ± 15 m^{-1} for tensile/compressive stress loading and a flat gasket pair with a curvature of $k = 0$ for normal package loading, where the latter was the control group.

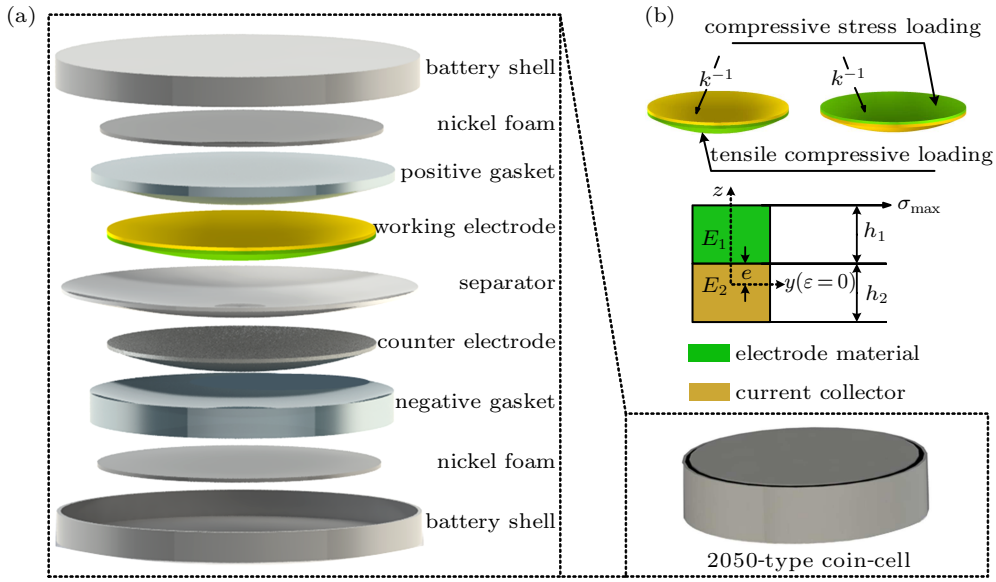


Fig. 1. Structure schematic diagram of (a) modified 2050-type coin-cell battery, in which working electrode is tensed, and (b) bending morphology and bilayer electrode structure under tensile/compressive stress loading.

Table 1. Three loading programs and stress loads of silicon composite electrode.

Loading program	Means	Curvature (m^{-1})	Maximum stress on electrode surface (kPa)
Tensile stress	contact with a positive gasket	$k=+45$	$+675\pm40.5$
		$k=+30$	$+450\pm27$
		$k=+15$	$+225\pm13.5$
Compressive stress	contact with a negative gasket	$k=-45$	-675 ± 40.5
		$k=-30$	-450 ± 27
		$k=-15$	-225 ± 13.5
Normal package (control group)	flat gasket pair	$k=0$	0

In the above experimental design, seven different tensile/compressive stresses were applied to the electrode. Here in this work, the stress was calculated by taking the normal packaging as a basis and reference; namely, under normal package loading the electrode underwent zero additional stress. Figure 1(b) shows a schematic of the electrode bending morphology under tensile/compressive stress loading and the corresponding bilayer structure that is comprised of electrode material and current collector. On the assumption that the bonded interface between the electrode material and current collector (*i.e.*, continuous interface deformation) is an ideal interface, according to the classical beam theory,[36–38] the stress in the electrode material, σ_1, and in the current collector, σ_2, are expressed as

$$\sigma_1 = E_1 z k, \quad e \le z \le h_1, \tag{1}$$

$$\sigma_2 = E_2 z k, \quad e - h_2 \le z \le e, \tag{2}$$

where E_1 and E_2 are the elastic modulus of the electrode material and the current collector, respectively; h_1 and h_2 are the thickness of the electrode material and the current collector, respectively; z is the distance offset from neutral layer; e is the distance from the neutral layer to the interface between the electrode material and the current collector; and k is the electrode bending curvature.

According to the static equilibrium condition for the electrode cross-section, we have[36–38]

$$\int_e^{h_1} \sigma_1 w \mathrm{d}z + \int_{e-h_2}^{e} \sigma_2 w \mathrm{d}z = 0, \tag{3}$$

where w is the width of the electrode.

Substituting Eqs. (1) and (2) into Eq. (3), the distance e from the neutral layer to the interface between the electrode material and the current collector can be obtained and expressed as

$$e = \frac{h_1+h_2}{2} \cdot \frac{1 - E_1 h_1^2 / E_2 h_2^2}{(1+h_1/h_2)(1+E_1 h_1 / E_2 h_2)}. \tag{4}$$

To facilitate the description of the load, the maximum stress on the electrode surface, σ_{max}, was used here. The value for σ_{max} was obtained by substituting Eq. (4) into Eq. (1), which is expressed as

$$\sigma_{max} = E_1 k \left(\frac{h_1+h_2}{2} \cdot \frac{1 - E_1 h_1^2 / E_2 h_2^2}{(1+h_1/h_2)(1+E_1 h_1 / E_2 h_2)} + h_1 \right). \tag{5}$$

2.2. Electrode material and electrochemical tests of LIBs

A highly-coupled high-specific-capacity silicon composite electrode was used in the experimental study. A copper foil with 10 μm in thickness was used as the current

collector, and a mixture of 70-wt% crystalline silicon particles (∼ 80 nm, Guangzhou Hongwu Material Technology Co., Ltd., China), 15-wt% super-P conductive additive (Timcal, Switzerland) and 15-wt% sodium alginate binder (18th Research Institute, Tianjin, China) was used as the electrode material. As illustrated in Fig. 1(a), the modified 2050-type coin-cell battery was assembled in a ZKX glove box (Nanjing Nanda Instrument Plant, China) filled with argon, where the prepared silicon composite electrode (diameter 15 mm, thickness 10 ± 1 μm) was the working electrode, metal lithium foil (∼ 450 μm, Tianjin Zhongneng Lithium Industry Co., Ltd., China) was the reference/counter electrode, porous polypropylene film (∼ 28-μm thick, Celgard Inc., USA) was the separator, and 1-M $LiPF_6$ in ethylene carbonate (EC) and dimethyl carbonate (DMC) (V:V of EC:DMC = 1:1) (Tianjin Jingniu, China) was the electrolyte solution. And then the electrode stress was calculated using Eq. (5), the geometric parameters and material parameters of the electrode as shown in Table 1. We used the seven maximum stresses of 675 ± 40.5, 450 ± 27, 225 ± 13.5, 0, -675 ± 40.5, -450 ± 27.5, and -225 ± 13.5 kPa, where the elastic modulus of the electrode material and current collector were 1 GPa and 70 GPa, respectively, according to the literature.[39,40] Here, the error range in stress came from fluctuation of 1 μm in electrode material thickness, and the affected degree was about 6%. For simplified description, the stress error was not shown below.

After battery assembly, the electrochemical experiments on silicon composite electrodes under seven stress conditions were carried out at room temperature. In the experiments, three samples were set under each stress loading condition to repeat the experiment and reduce error. Four types of electrochemical tests were carried out to obtain different performance parameters. (i) To determine the effect of tensile/compressive stress on the cyclic performance, a constant current charging–discharging test was performed (where discharging corresponds to lithiation and charging to delithiation) to obtain the potential, capacity, coulombic efficiency and dissipation as a function of cycle number. (ii) To determine the effect of tensile/compressive stress on the electrochemical activity and reversibility, a CV test was conducted after the 3rd and 10th charging–discharging cycles to obtain the CV curves. (iii) To determine the effect of tensile/compressive stress on the electrochemical migration and reaction, an EIS test was carried out in the 10th lithiation process and under different cycles to obtain the Ohmic impedance R_s, the membrane impedance of the solid electrolyte interface (SEI) R_{SEI}, and the charge transfer impedance R_{ct}. (iv) To determine the effect of tensile/compressive stress on the electrochemical diffusion, a GITT test in the 10th lithiation process was performed to obtain the diffusion coefficient D_s. Table 2 displays the measurement conditions, measurement instruments, and corresponding measurement parameters of these four types of electrochemical tests.

Table 2. Purposes, conditions, instruments, and parameters of four electrochemical technologies.

Measurement technology	Measurement purpose	Measurement condition	Measurement instruments	Measurement parameters
Constant current (dis) charging	stress effect on cycle performance	rate C/5; potential 2 V *versus* ∼ 0.01 V;	LAND-CT2001A battery tester	potential curves; cycled capacity; cycled dissipation; Coulombic efficiency;
CV	stress effect on activity and reversibility	voltage interval 0.01 V–1.5 V; scanning speed 0.1 $mV \cdot s^{-1}$;	Chi660A electrochemical workstation	CV curves;
EIS	stress effect on migration and reaction	relaxation 15 min; frequency 100 kHz–20 mHz; amplitude ±5 mV;	Chi660A electrochemical workstation	R_s; R_{SEI}; R_{ct};
GITT	stress effect on diffusion	pulse current C/5; pulse time 10 min; relaxation 30 min	LAND-CT2001A battery tester	diffusion coefficient D_s;

3. Cycle performance and experimental analysis of silicon composite electrode under stress loading

The electrochemical performance typically includes the two parts, *i.e.*, cycle performance and kinetics performance, where the former is directly related to the battery life. In this section, the cycle performances of silicon composite electrodes under different tensile/compressive stresses were demonstrated, including the cycle specific capacity, the coulombic efficiency, the capacity retention rate, the energy dissipation ratio, and the cycle impedance spectrum. Using these data, the stress influence mechanism was analyzed.

The specific capacity of an electrode material relates to its ability to store Li, which is the most basic parameter to characterize the electrode cycle performance. A higher specific capacity in the cycle process corresponds to a slower degradation and a superior cycle performance. Figures 2(a) and 2(b) show the discharging capacity and charging capacity of silicon composite electrodes as a function of the cycle number during C/5 constant-current lithiation–delithiation cycles under seven different stress values for three loading programs of

tensile/compressive stress loading and normal package loading, respectively and the corresponding coulombic efficiency curves are shown in Fig. 2(c). It can be found that the decay rate of the capacity is rapid in the early cycles with a smaller coulombic efficiency, and the effect of stress on the capacity is not obvious. With the increase of cycle number, however, the capacity decay rate is gradually reduced and the effect of the tensile stress and the compressive stress become evident, where the largest capacity and coulombic efficiency were measured under tensile stress loading, followed by the normal package loading, and then the smallest capacity and coulombic efficiency under compressive stress loading. In addition, a larger stress load induced a more significant effect. To eliminate errors caused by electrode difference, the capacity retention rate (*i.e.*, the ratio of cycled discharging capacity to the first discharging capacity) was used to further characterize cycle performance stability. Figure 2(d) shows the capacity retention rate of silicon composite electrodes as a function of cycle number at later cycles under tensile/compressive stress loading and normal package loading. Like the results for specific capacity, tensile stress loading increased the capacity retention rate of silicon composite electrodes and reduced the decline compared with normal package loading, while compressive stress reduced the capacity retention rate and accelerated the decline. These data indicate that a tensile stress enhanced capacity and benefited the silicon composite electrode during cycling, while compressive stress weakened the capacity and impaired the electrode during cycling. The weakening effect of the compressive stress was more obvious than the enhancing effect of the tensile stress. Taking the 30th cycle for example, a 450-kPa tensile and compressive stress caused the capacity retention rate to respectively increase by 1.1% and decrease by 2.7%. We note that a small stress induced a significant difference in cycle performance. Further, current research shows that compressive stress on the silicon composite electrode during the electrochemical cycle was about 9 MPa.[11,39] This indicates that the stress-based electrochemical performance regulation is critical.

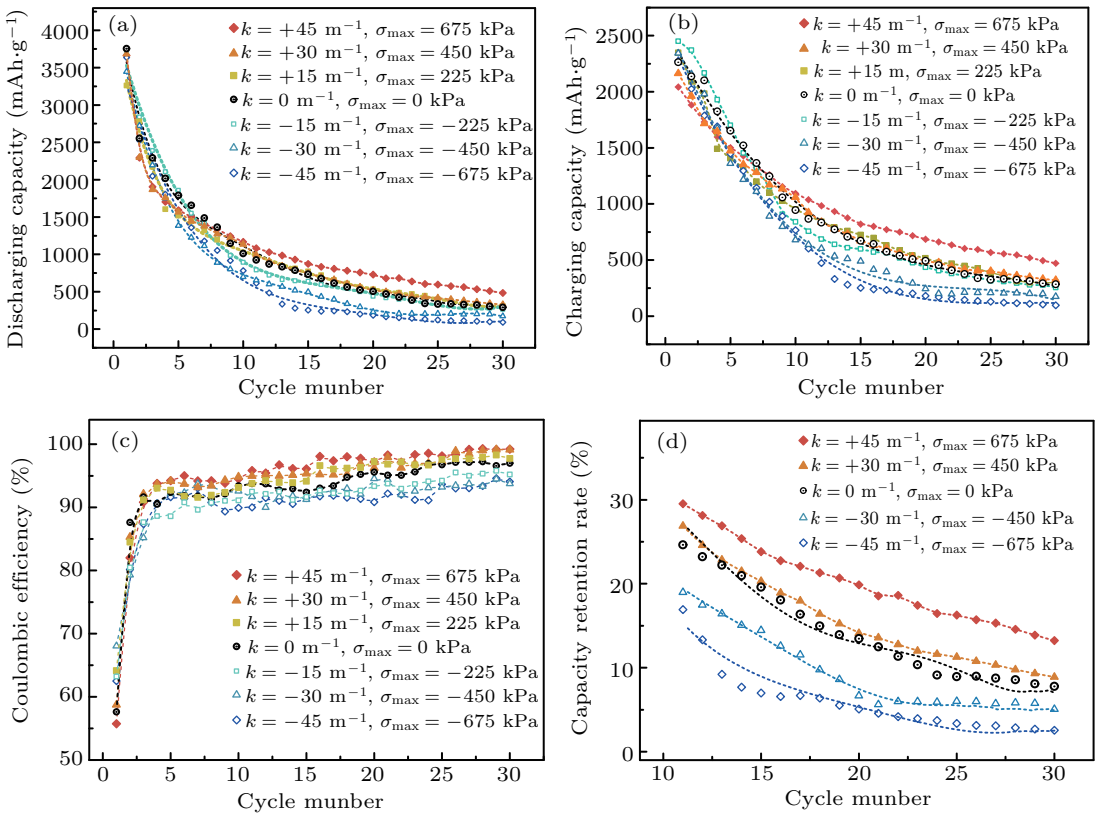


Fig. 2. (a) Discharging specific capacity, (b) charging specific capacity, (c) Coulombic efficiency, and (d) capacity retention rate of silicon composite electrodes as a function of cycle number under tensile/compressive stress loading and normal package loading.

Electrochemical charging and discharging contain an energy conversion process involving electrical and chemical energy, and thus energy dissipation is inevitable. Here, energy dissipation was used to evaluate the cycle performance, where a lower energy dissipation indicates a better cycle performance. In particular, charging is an energy storage process that converts electrical energy into chemical energy, while discharging is an energy output process that converts chemical energy into electrical energy. Therefore, the energy dissipation was obtained by subtracting the quantity of discharged electrical energy from the quantity of charged electrical energy. Energy dissipation was therefore a product of the current and the area within the potential–time hysteresis curve of the constant-current charging–discharging experiment. The

energy dissipation ratio of silicon composite electrodes *versus* the cycle number (where the cycle was run at a C/5 charging-discharging rate) under seven different stress values of tensile/compressive stress loading and normal package loading is shown in Fig. 3(a). The dissipation ratio was defined as the energy dissipation over the total energy, thus excluding the influence of electrode variation. Like the results found for the capacity retention rate, the effect of the stress on energy dissipation early in the cycles is not obvious, but as the cycle number increases the effect of stress loading gradually appears. For a clearer display of the impact trend, figure 3(b) shows the dissipation ratio during the 30th cycle as a function of stress, which exhibits a dissipation ratio decreasing with tensile stress loading increasing and the ratio increases with compressive stress loading increasing. These data indicate that a tensile stress enhanced the energy conversion rate and benefited the silicon composite electrode during cycling, while compressive stress impaired the electrode during cycling. In addition, the harmful effect of the compressive stress was more apparent than the beneficial effect of the tensile stress. Taking the 30th cycle for example, a 675-kPa tensile and compressive stress respectively reduced the dissipation ratio by about 1% and increased it by 5%.

In addition, previous research has reported that the electrode impedance increases and specific capacity decreases with cycle increasing.[31,41,42] This signifies that impedance is also a useful parameter for characterizing electrode cycle performance, where a larger resistance corresponds to an impaired cycle performance. Figure 4 shows a standard impedance spectrum (on the right side, featuring two semicircles and a line) and the electrochemical reaction process (on the left side) of a silicon electrode. Combining these two plots, the information contained in and correlation between impedance and reaction can be described, and is divided into four parts:[43] (I) The intersection between the high-frequency of the impedance spectrum and the real axis is called the ohmic impedance, R_s, which corresponds to the process of electron and ion migrating through the electrode structure comprising the electrode, electrolyte and separator. (II) The high-frequency semicircle of the impedance spectrum is called the membrane impedance of the SEI, R_{SEI}, corresponding to the process of ion migration through the SEI film on the silicon particle surface. (III) The high–middle-frequency semicircle of the impedance spectrum is called the charge transfer impedance R_{ct}, which corresponds to the process of electron/ion transfer and binding at the interface between the silicon particles and the SEI film. (IV) The low-frequency line of the impedance spectrum is called the diffusion impedance Z_w, corresponding to the process of ion diffusion inside the silicon particles.

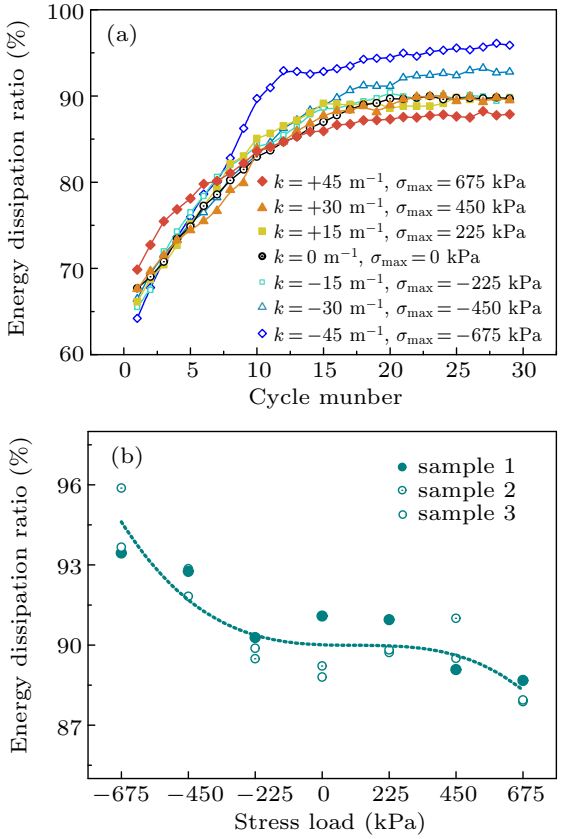


Fig. 3. (a) Energy dissipation ratios of silicon composite electrodes varying with cycle number under tensile/compressive stress loading and normal package loading. (b) Energy dissipation ratio *versus* stress during the 30th cycle.

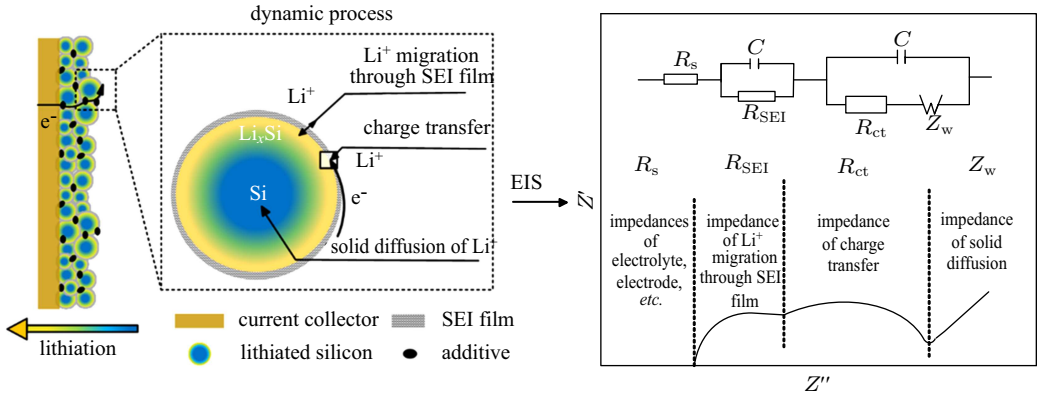


Fig. 4. Schematic diagram of electrochemical reaction process and standard impedance spectrum of a silicon electrode.[43]

Figures 5(a) and 5(b) show the impedance spectra of silicon composite electrodes after 3 cycles and 30 cycles, respectively, in a frequency range from 20 mHz to 100 kHz under maximum tensile/compressive stress loading and normal package loading. The spectra clearly show that ohmic resistance, R_s, SEI film resistance, R_{SEI}, and charge transfer resistance, R_{ct} increase as the cycle number increases, echoing the decrease of specific capacity with cycle number increasing. And after cycling, the three resistances reach the maximum values under compressive stress and the minimum values under tensile stress. For quantitative analysis of the resistances, the impedance spectra under varying stress loading were fitted via an equivalent circuit model (see the inset in Figs. 5(a) and 5(b)). Here, the impedance increment ratio, $\Delta\bar{R}$, relative to the third cycle, is shown in Fig. 5(c). Inspection of Figs. 5(a)–5(c) shows that as the stress loading varies, the tensile stress leads these three impedance values to decrease while the compressive stress causes R_s, R_{SEI}, and R_{ct} to increase. Further, the increasing effect of the compressive stress is more obvious than the decreasing effect of the tensile stress. For example after 30 cycles, under a 675-kPa tensile and compressive stress, the value of $\Delta\bar{R}_s$ decreases by 13.4% and increases by 18.3%, respectively; the value of $\Delta\bar{R}_{SEI}$ decreases by 5.7% and increase by 24.8%, respectively; and the value of $\Delta\bar{R}_{ct}$ decreases by 17.8% and increases by 21.1%, respectively. These data demonstrate that the tensile stress can enhance electron and ion transport, which is beneficial to the cycle; while the compressive stress has an opposite effect.

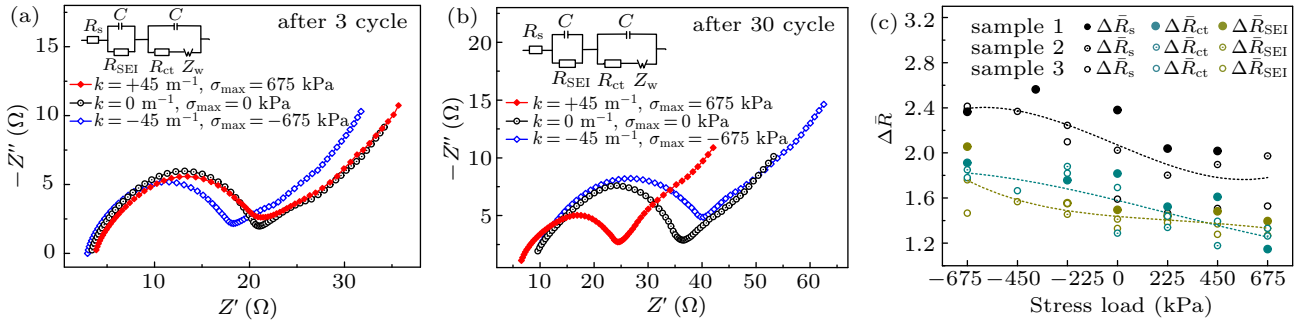


Fig. 5. Impedances of silicon composite electrodes. Electrochemical impedance spectra after (a) 3 cycles and (b) 30 cycles under maximum tensile/compressive stress loading and normal package loading. (c) Impedance increments of $\Delta\bar{R}_s$, $\Delta\bar{R}_{SEI}$, and $\Delta\bar{R}_{ct}$ *versus* stress loading, where increment refers to the impedance ratio relative to that of the third cycle.

Table 3. Cycle performance parameters of silicon composite electrode at the 30th cycle under tensile/compressive stress loading and normal package loading.

Maximum stress (kPa)	Capacity (mAh·g^{-1})	Capacity retention rate (%)	Dissipation ratio (%)	Impedance increment		
				$\Delta\bar{R}_s$	$\Delta\bar{R}_{SEI}$	$\Delta\bar{R}_{ct}$
–675	93	2.6%	95%	2.39	1.76	1.84
–450	174	5.1%	93%	2.36	1.57	1.66
–225	265	7.1%	90%	2.31	1.52	1.81
	291	7.8%	90%	2.02	1.41	1.52
225	323	9.5%	90%	1.83	1.41	1.43
450	327	8.9%	91%	1.87	1.37	1.39
675	484	13.2%	89%	1.75	1.33	1.25

Taking the 30th cycle for example, in Table 3 summarized are some experimental results of the cycle performance of silicon composite electrodes under seven tensile/compressive stress loads. The results demonstrate a nonlinear effects of enhancement and inhibition on cycle performance under the tensile and compressive stress, respectively. The results exhibit a higher specific capacity, a higher capacity retention rate, a lower energy dissipation rate and a lower impedance under tensile stress loading; and the opposite phenomena under compressive stress loading. In the following we analyzed the mechanism whereby the stress influenced cycle performance, including two aspects. i) The silicon composite electrode exhibits a bilayer structure comprising a current collector and an electrode material layer, where the latter is a porous film. In the electrochemical process, the limitation of the current collector caused a limited electrode material expansion, thereby inducing the electrode damage including cracks in the electrode material and electrode material/current collector interface debonding.[3,44] Stress loading changed the electrode physical morphology. Tensile stress conditions gave rise to looser microstructural pores of the electrode material and smaller deformation of the electrode material via particle expansion in the lithiation–delithiation process. This resulted in a smaller restriction of the current collector, and thus phenomena such as electrode material cracks and islands and bilayer interface debonding were mitigated. This was consistent with the minimum $\Delta\bar{R}_s$ and $\Delta\bar{R}_{ct}$ value under tensile stress found in the experimental measurements. Thus, the degree of macro-

scopic damage to the electrode was reduced, and the cycle performance was enhanced. On the contrary, all these were found to be the opposite under compressive stress conditions, where the degree of macroscopic damage to the electrode was increased and the cycle performance was weakened. ii) Particle deformation in the electrochemical process caused the silicon particles to come into contact and extrude. This generated mechanical energy dissipation to resist the deformation, which affected the energy dissipation ratio. The physical morphology was changed by stress loading, affecting the lithiation and the expansion condition of the particles. Under tensile stress loading, the looser electrode material provided more spaces for particle expansion in the lithiation–delithiation process, thus reducing contact compressive stress and mechanical energy dissipation. This would lower the energy dissipation ratio, which is consistent with experimental result, and will enhance the cycle performance. On the contrary, compressive stress conditions increased the mechanical energy dissipation and the energy dissipation ratio, thus weakening the cycle performance.

The above experimental results demonstrate that the cycle performance of silicon composite electrodes was enhanced by tensile stress and inhibited by compressive stress. The influence mechanism took it into consideration that stress loads changed the physical and mechanical properties of the electrode material microstructure. Tensile stress loading increased the microstructural pores of the electrode material and mitigated electrode damage (*i.e.*, electrode material cracks and interface debonding) and mechanical energy dissipation caused by particle contact and extrusion.

4. Kinetics performance and experimental analysis of silicon composite electrode under stress loading

As mentioned above, the electrochemical performance includes both cycle performance and kinetics performance. The above results demonstrate that a tensile stress enhances the cycle performance, which is closely related to the kinetics performance. In the following, we primarily demonstrate the effect of stress on the kinetics performance of silicon composite electrodes, including the electrode activity and polarization (obtained from CV and potential hysteresis data), ion migration and reaction (obtained from impedance spectra), and diffusion (obtained from GITT potential data). Then, we analyze the influence mechanism based on the experimental data.

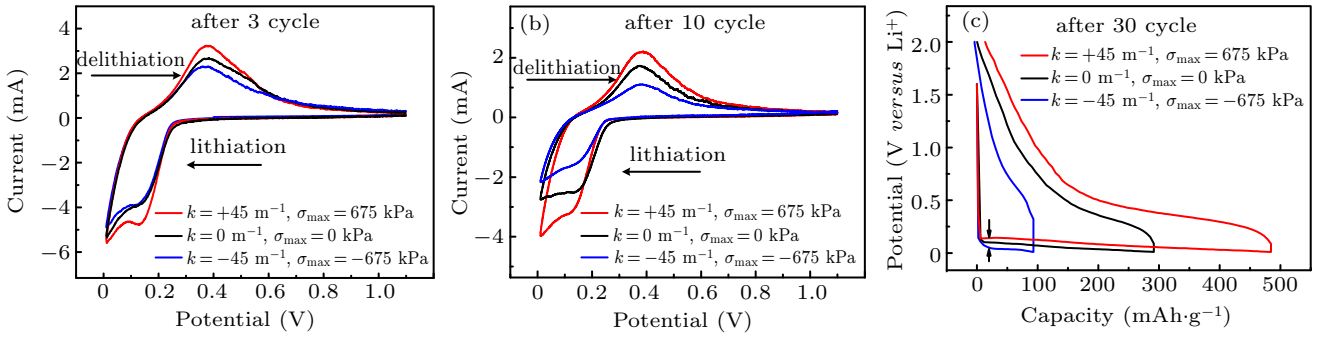


Fig. 6. CV curve after (a) 3 cycles and (b) 10 cycles, and (c) potential hysteresis curve at the 30th cycle of silicon composite electrodes under maximum tensile/compressive stress loading and normal package loading.

Electrochemical activity and polarization are inseparable from the cycle performance, where a higher activity corresponds to a higher lithium storage capacity and a smaller polarization loss corresponds to a higher energy conversion rate.[35,45] The CV method is effective for studying electrochemical activity, and current–potential curves contain the following information.[35,41,46,47] A smaller potential difference between the lithiation reduction peak and delithiation oxidation peak indicates a better reaction reversibility. Also, a higher current at the peak position indicates a better reaction activity and stronger reaction ability. Figures 6(a) and 6(b) show the CV curve of silicon composite electrodes after 3 cycles and 10 cycles, respectively, at a scan rate of 0.1 mV·s^{-1} under maximum tensile/compressive stress loading and normal package loading. Comparing with the normal package loading, a higher current at the peak position and a smaller peak potential difference are found under the tensile stress condition, while a lower current at the peak position and a greater peak potential difference are found under the compressive stress condition in Figs. 6(a) and 6(b). This indicates that a tensile stress enhances the reactivity, reaction ability and reversibility, while a compressive stress yields the opposite result. Additionally, the potential hysteresis curve is an effective basis to determine the degree of electrode polarization. This is generally described as the overpotential, which is the difference between the real-time potential and equilibrium potential, where a larger overpotential relates to a greater polarization. Figure 6(c) shows the potential hysteresis curves at the 30th cycle of silicon composite electrodes under maximum tensile/compressive stress loading and normal package loading. Comparing with the normal package loading, the potential decreases and the overpotential increases under com-

pressive stress loading, while the potential increases and overpotential decreases under tensile stress loading. This demonstrates that a tensile stress reduces the degree of polarization and polarization loss, while a compressive stress has an opposite effect. These kinetic performance measurement results are consistent with the cycle performance results wherein a tensile stress enhances and a compressive stress inhibits the cycle performance.

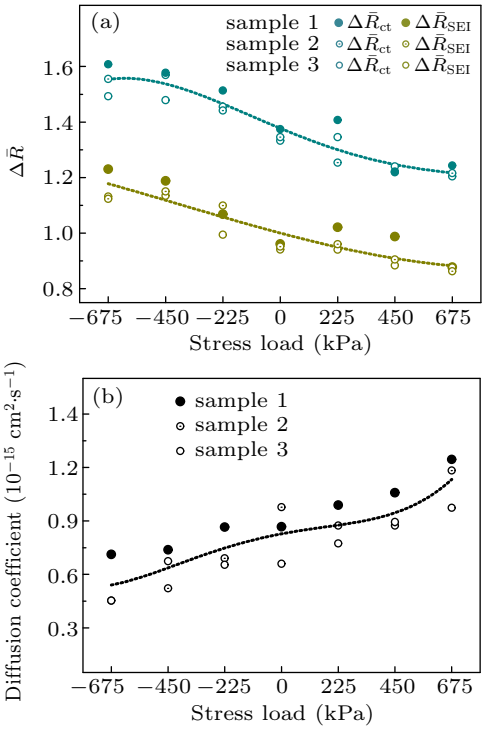


Fig. 7. Average values of (a) charge transfer impedance, $\Delta\bar{R}_{ct}$, and SEI film impedance, $\Delta\bar{R}_{SEI}$, and (b) diffusion coefficient, $\bar{D}_S$, of three silicon composite electrode samples at the 10th lithiation process as a function of tensile/compressive stress loading.

The migration of ions and electrons, their diffusion and reaction are also closely related to cycle performance. Smoother kinetic processes correspond to less internal electrode damage, smaller degree of polarization, and greater stability. As mentioned above, the EIS is an effective means to measure the migration and reaction, containing the measure of the film impedance, R_{SEI}, to describe ion migration through the SEI film as well as the charge transfer resistance, R_{ct}, to describe electron and ion transfer at the silicon particle/SEI film interface. The smaller values for the R_{SEI} and R_{ct} resistance signify an easier migration and reaction process. Taking the 10th lithiation cycle for example, figure 7(a) shows the average resistance values ($\Delta\bar{R}_{SEI}$ and $\Delta\bar{R}_{ct}$) with varying tensile/compressive stress load for three silicon composite electrode samples, and the corresponding $\Delta\bar{R}_{SEI}$ and $\Delta\bar{R}_{ct}$ values under seven different stress loads are given in Table 4. The results show that the R_{SEI} and R_{ct} impedance decrease nonlinearly under an increasing tensile stress load and increase nonlinearly under an increasing compressive stress load, where the effect of the compressive stress is more obvious than that of the tensile stress. For example, for a stress load of 675 kPa, the $\Delta\bar{R}_{SEI}$ decreases by 8.4% and increases by 22.1% under tensile and compressive stress, respectively, and $\Delta\bar{R}_{ct}$ decreases by 9.6% and increases by 14.8%, respectively. The data demonstrate that a tensile stress enhances the electron and ion transport, while a compressive stress has an opposite effect. In addition, the diffusion coefficient is typically used to characterize the diffusion process, where larger diffusion coefficient corresponds to more rapid ion diffusion inside particles. Figure 7(b) shows the average diffusion coefficient value, $\bar{D}_S$, as a function of tensile/compressive stress load of three silicon composite electrode samples at the 10th lithiation process obtained by the GITT method, and the corresponding $\bar{D}_S$ values under seven different stress loads are given in Table 4. It is shown that the tensile stress increases the diffusion coefficient nonlinearly, while the compressive stress nonlinearly reduces $\bar{D}_S$. Taking a 675-kPa stress load for example, a tensile stress increases the diffusion coefficient by 32.5%, while a compressive stress reduces it by 35%. This indicates that the tensile stress promotes the diffusion while the compressive stress inhibits the diffusion.

Table 5. Average values of two impedances and diffusion coefficient of silicon composite electrode under tensile/compressive stress loads at the 10th lithiation process.

Maximum stress (kPa)	$\Delta\bar{R}_{SEI}$	$\Delta\bar{R}_{ct}$	$\bar{D}_S$ (10^{-16} cm^2·s^{-1})
–675	1.55	1.16	5.4
–450	1.54	1.15	6.4
–225	1.47	1.05	7.4
	1.35	0.95	8.3
225	1.34	0.97	8.8
450	1.23	0.93	9.4
675	1.22	0.87	11

The above experimental results demonstrate that a tensile stress enhances the kinetic performances of silicon composite electrodes, characterized by a larger reactivity, a stronger reaction ability, a better reversibility, a smaller polarization, a faster ion and electron migration, and a higher diffusion coefficient. Contrarily, a compressive stress has an opposite effect. According to these experimental results, in the following we analyze the regulation that the stress may have on the kinetic performance, primarily including two aspects. I) Previous reports have shown that a compressive stress limits the diffusion and reaction inside active material, leading to a higher concentration gradient inside the particles. This affects the stress distribution and induces a larger stress gradient, ultimately resulting in particle fracture.[2,7,10,22,25,26,29] Under tensile stress conditions, the microstructural pores in the electrode material increase. This provides more channels and pathways for transporting and migrating the ions and electrons, therefore enhancing the ion migration performance, charge transfer process, and diffusion performance. This reduces the accumulation of ions and electrons on the particle surface and results in a more

uniform Li concentration distribution and a more complete reaction inside particles. This analysis is shown in Fig. 8, and it is consistent with the decrease of the experimentally-measured $\Delta\bar{R}_{\mathrm{SEI}}$ and $\Delta\bar{R}_{\mathrm{ct}}$ impedances under tensile stress. In this condition, the lithiation-induced deformation is more uniform and the compressive stress and the stress gradient inside the particles are relieved. Therefore, the SEI film cracking and particle fracturing reduced, resulting in a lesser degree of particle damage and thus enhancing the electrochemical performance. On the contrary, the effect of a compressive stress is the opposite. Under this condition, diminished diffusion and reaction via the reduced porous structure increase the compressive stress and the stress gradient inside the particles. This leads the particle damage to increase and thus a electrochemical performance to weaken. II) The electrochemical reaction is related to the overpotential, where a larger overpotential indicates an increased amount of energy required for reaction. Thus, a larger overpotential is prohibitive for the proceeding reaction, resulting in a greater polarization dissipation. As mentioned before, ion/electron diffusion and reaction are enhanced under tensile stress loading, indicating a smaller overpotential. This is consistent with the experimental measurement shown in Fig. 6(c), and thereby increasing the time to reach the cut-off voltage and specific capacity, and reducing the polarization energy dissipation. This reduces the energy dissipation ratio and improves the electrochemical performance. On the contrary, a compressive stress increases the overpotential and the polarization dissipation, thus weakening the electrochemical performance.

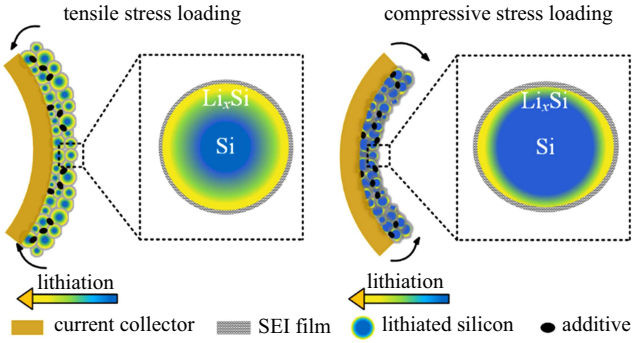


Fig. 8. Schematic diagram of lithiated silicon composite electrode under tensile/compressive stress loading.

The above experimental results demonstrate that a tensile stress promotes the kinetic performance of a silicon composite electrode, while a compressive stress weakens it. The influence mechanism of this effect is that the stress loads change the electrical, chemical, and mechanical properties of the electrode material microstructure. Tensile stress loading provides more ion and electron migration channels, enhancing the electron and ion transport abilities, promoting diffusion and a more uniform distribution of lithium ions inside the silicon particles, alleviating the stress and stress gradient inside the silicon particles, and reducing the damage and fracture of silicon particles and the polarization dissipation.

5. Conclusions

Stress plays an important role in determining the battery cycle performance, life, and safety. In this paper, we investigated the difficulties in experiments on the stress-affected performance of LIBs. A stress loading device is designed and seven different tensile/compressive stresses are applied to the electrodes through an active stress loading method. In this way, tensile/compressive stress loading is realized and its effect is decoupled from the electrochemical process. The electrochemical experiments of LIBs under varying tensile/compressive stress loading are performed on a silicon composite electrode by using four types of electrochemical tests.

The above experiments under seven tensile/compressive loads with three samples at each load quantify the influences of tensile stress and compressive stress on cycle performance and kinetics performance. It is shown that tensile stress loads correspond to a higher specific capacity and capacity retention rate, a smaller energy dissipation rate and resistance, a better reactivity and reaction ability, a smaller polarization, a faster ion and electron migration, and a higher diffusion coefficient. A compressive stress, however, exhibits the opposite effects. Taking the average diffusion coefficient $\bar{D}_{\mathrm{S}}$ for example, a tensile stress of 675 kPa increases $\bar{D}_{\mathrm{S}}$ by 32.5%, while an equivalent compressive stress decreases $\bar{D}_{\mathrm{S}}$ by 35%. All the experimental results obtained from the three samples under seven tensile/compressive stress loads demonstrate that stress significantly affects cycle performance and kinetics performance, and the influence is nonlinear.

Further, the stress influence mechanism on electrochemical performance is analyzed from an experimental viewpoint, and it is found to primarily originate from the deformation, stress, damage, and energy dissipation of electrode materials. Tensile stress increases the microstructural pores in electrode material for deformation, alleviating the compressive stress caused by silicon particle expansion during the electrochemical reaction, improving the ion and electron migration, promoting the diffusion and reaction inside the particles, and reducing the degree of electrode damage, and energy dissipation. However, a compressive stress has an opposite effect, demonstrating an increase in particle extrusion deformation, particle contact compressive stress, degree of electrode damage, and energy dissipation. The essence in the influence of the stress enhancement on the electrochemical performance is therefore the improvement and optimization of the diffusion, reaction, and stress in the microstructure of electrode material as well as their interactions.

The experimental results herein confirm an enhanced regulation effect of tensile stress on electrochemical performance of LIBs. In fact, the mechano–electrochemical coupling effect is widely present in energy storage and conversion pro-

cess, and not only in LIBs. Therefore, the results in this paper promote the application of mechanical load in lifetime optimization of energy storage devices. For example, pre-loading various stresses or cleverly avoiding stress during the working operation can be an effective means of energy storage regulation of energy materials.

References

[1] Ebner M, Marone F, Stampanoni M and Wood V 2013 *Science* **342** 716
[2] Zhang X Y, Chen H S and Fang D 2020 *Int. J. Mech. Sci.* **169** 105323
[3] Jangid M K and Mukhopadhyay A 2019 *J. Mater. Chem. A* **7** 23679
[4] Zhu T 2016 *Chin. Phys. B* **25** 014601
[5] Hofmann T, Westhoff D, Feinauer J, Andrä H, Zausch J, Schmidt V and Müller R 2020 *Int. J. Solids Struct.* **184** 24
[6] Palacin M R and de Guibert A 2016 *Science* **351** 1253292
[7] Zhang Y and Guo Z 2018 *Acta Mech. Sin.* **34** 706
[8] Xie H, Song H, Guo J G, Kang Y, Yang W and Zhang Q 2019 *Carbon* **144** 342
[9] Zuo P and Zhao Y P 2016 *Extreme Mechanics Letters* **9** 467
[10] Ji L and Guo Z 2018 *Acta Mech. Sin.* **34** 187
[11] Xie H, Zhang Q, Song H, Shi B and Kang Y 2017 *J. Power Sources* **342** 896
[12] Yang W, Xie H, Shi B, Song H, Qiu W and Zhang Q 2019 *J. Power Sources* **423** 174
[13] Hou J, Qu S, Yang M and Zhang J 2020 *J. Power Sources* **450** 227697
[14] Feng K, Li M, Liu W, Kashkooli A G, Xiao X, Cai M and Chen Z 2018 *Small* **14**
[15] Hernandez C R, Etiemble A, Douillard T, Mazouzi D, Karkar Z, Maire E, Guyomard D, Lestriez B and Roué L 2018 *Adv. Energy Mater.* **8** 1701787
[16] Wang L, Duan X, Liu B, Li Q M, Yin S and Xu J 2020 *J. Power Sources* **448** 227468
[17] Zhu T, Fang X, Wang B, Shen S and Feng X 2019 *Sci. China: Technol. Sci.* **62** 1385
[18] Zhao Y, Stein P, Bai Y, Al-Siraj M, Yang Y and Xu B X 2019 *J. Power Sources* **413** 259
[19] Eshghinejad A and Li J 2015 *Mech. Mater.* **91** 343
[20] Zhang Q, Tang C and Fu L 2019 *Appl. Surf. Sci.* **497** 143723
[21] Zhang K, Li Y, Wang F, Zheng B and Yang F 2019 *Appl. Phys. Express* **12** 045004
[22] Jin C, Li H, Song Y, Lu B, Soh A K and Zhang J 2019 *Sci. China: Technol. Sci.* **62** 1357
[23] Burebi Y, Zheng J and Qu S 2019 *Sci. China: Technol. Sci.* **62** 1365
[24] Lu Y, Zhang P, Wang F, Zhang K and Zhao X 2018 *Electrochim. Acta* **274** 359
[25] Gao X, Lu W and Xu J 2020 *J. Power Sources* **449** 227501
[26] McDowell M T, Ryu I, Lee S W, Wang C, Nix W D and Cui Y 2012 *Adv. Mater.* **24** 6034
[27] Lee S W, Lee H W, Ryu I, Nix W D, Gao H and Cui Y 2015 *Nat. Commun.* **6** 7533
[28] Gu M, Yang H, Perea D E, Zhang J G, Zhang S and Wang C M 2014 *Nano Lett.* **14** 4622
[29] Yang H, Liang W, Guo X, Wang C M and Zhang S 2015 *Extreme Mechanics Letters* **2** 1
[30] Piper D M, Yersak T A and Lee S H 2012 *J. Electrochem. Soc.* **160** A77
[31] Ratyński M, Hamankiewicz B, Krajewski M, Boczar M and Czerwiński A 2018 *RSC Adv.* **8** 22546
[32] Cannarella J and Arnold C B 2014 *J. Power Sources* **245** 745
[33] Wuensch M, Kaufman J and Sauer D U 2019 *J. Energy Storage* **21** 149
[34] Müller V, Scurtu R G, Memm M, Danzer M A and Wohlfahrt-Mehrens M 2019 *J. Power Sources* **440** 227148
[35] Xie H M, Guo J G, Song H B, Shi B Q and Kang Y L 2018 *Energy Technol.* **6** 1788
[36] Lemaitre J, Chaboche J L and Maji A K 1992 *J. Eng. Mech.* **119** 642
[37] Wang S B and Kang Y L 2007 *Mechanics of Materials* (Beijing: Higher Education Press) pp. 145–146 (in Chinese)
[38] Gere J M, Timoshenko S P and Saunders H 1984 *J. Vib. Acoust.* **108** 483
[39] Xie H M, Kang Y L, Song H B and Zhang Q 2019 *J. Power Sources* **424** 100
[40] Xie H M, Kang Y L, Song H B, Guo J G and Zhang Q 2020 *Acta Mech. Sin.*
[41] Zeng W, Xing J, Chen J C M, Ng K Y S, Oshihara K and Cheng M M C 2018 *Electrochim. Acta* **281** 282
[42] Mussa A S, Klett M, Lindbergh G and Lindström R W 2018 *J. Power Sources* **385** 18
[43] Barsoukov E, Kim J H, Kim J H, Yoon C O and Lee H 1999 *Solid State Ionics Diffusion & Reactions* **116** 249
[44] Lu B, Ning C Q, Shi D X, Zhao Y F and Zhang J Q 2020 *Chin. Phys. B* **29**
[45] Çapraz Ö Ö, Rajput S, White S and Sottos N R 2018 *Exp. Mech.* **58** 561
[46] Jiang Y, Mu D, Chen S, Wu B, Cheng K, Li L and Wu F 2016 *J. Power Sources* **325** 630
[47] Dai C, Li C, Huang H, Wang Z, Zhu X, Liao X, Chen X, Pan Y and Fang D 2019 *Solid State Ionics* **331** 56